Constant-stress Hugoniostat method for following the dynamical evolution of shocked matter

R. Ravelo,[1,2] B. L. Holian,[3] T. C. Germann,[2] and P. S. Lomdahl[3]
[1]*Physics Department and Materials Research Institute, University of Texas, El Paso, Texas 79968, USA*
[2]*Applied Physics Division, Los Alamos National Laboratory, Los Alamos, New Mexico 87545, USA*
[3]*Theoretical Division, Los Alamos National Laboratory, Los Alamos, New Mexico 87545, USA*
(Received 26 November 2003; revised manuscript received 4 March 2004; published 16 July 2004)

We present an alternative equilibrium molecular dynamics method—the uniaxial constant-stress Hugoniostat—for following the dynamical evolution of condensed matter subjected to shock waves. It is a natural extension of the recently developed uniaxial constant-volume Hugoniostat [Maillet *et al.*, Phys. Rev. E **63**, 016121 (2001)]. Integral feedback is employed to reach the Hugoniot (final) state of the shock process by controlling both the normal component of the stress tensor and internal energy. The finite strain rate imposed on the system is closely related to that inherent in the front of a shock wave. The method can easily identify phase transitions along the Hugoniot shock states, even those that exhibit multiple wave structures. As an example of the method, we have simulated the Hugoniot of a Lennard-Jones crystal shocked along the ⟨110⟩ direction. The results agree well with multi-million-atom nonequilibrium molecular-dynamics simulations.

DOI: 10.1103/PhysRevB.70.014103 PACS number(s): 64.10.+h, 02.70.Ns, 62.50.+p, 62.20.Fe

I. INTRODUCTION

The study of material behavior under shock-loading conditions has been actively pursued for almost a century. In the 1970s, the first computer experiments of shock waves in solids demonstrated that nonequilibrium molecular dynamics (NEMD) simulations can be a powerful tool to study the dynamics of shock propagation in solids and liquids.[1,2] From those early days, the field of NEMD simulations of shock phenomena has advanced to the point where the study of shock-induced plasticity,[3] phase transitions,[4] and detonations[5] in single crystals is now possible, employing systems as large as several hundred million atoms. Despite this enormous progress, NEMD simulations of shock waves remain a computationally intensive undertaking, requiring ever larger systems in order to probe longer time scales, or as in the case of polycrystalline materials of even submicron size grains, systems larger than what is currently possible in order to achieve steady shock profiles.[6]

Recent advances in experimental techniques, especially in the areas of laser-shock processing (LSP) and *in situ* time-resolved x-ray diffraction and photoelectron spectroscopy, have dramatically increased the spatial and temporal resolution of shock-loaded experiments, allowing the study of lattice structures and material response on subnanosecond time scales. At the same time, advances in massively parallel computer simulations have allowed the investigation of planar shocks at length and times scales that are approaching those in current computational techniques. As a result, simulations and experiments are converging, in particular in the area of single-crystal plasticity and deformation. For instance, experiments on LiF single crystals have revealed marked differences in the yield stress as a function of shock direction.[7] This orientational dependence is also observed in large-scale NEMD simulations of shock propagation in defect-free fcc crystals.[8] Recent laser-driven shock experiments of Cu(100) single crystals indicate that the observed dislocation generation and defect structure is consistent with loop nucleation and growth at the shock front.[9] This finding is also in agreement with NEMD simulations of shock propagation in fcc(100) crystals.[3,10,11] However, NEMD simulations are currently limited to time scales of tens of picoseconds, and probing longer times is important in order to make a more direct comparison with current experiments.

Several dynamical approaches have emerged recently as alternatives to traditional NEMD, aimed at extracting dynamical and structural information, using smaller system sizes to allow the study of longer-time processes. One such approach is the "ramjet" or "moving window".[12] This is a NEMD method where a region around the shock front is followed in time by moving the computational cell at the shock-wave speed. As long as the shock front is steady, the method allows accurate determination of shock profiles with much smaller system sizes than traditional NEMD. By employing time averaging, it can provide accurate information of nonequilibrium thermodynamic quantities as a function of distance from the shock front. The method, by construction, cannot be used to follow multiwave structures, such as those produced in mixed-phase regions of the Hugoniot.

A recently developed equilibrium molecular-dynamics method aims at reproducing the final state of the compressed material after the shock wave has passed through. In this method, termed the "uniaxial Hugoniostat,"[13] the system is instantaneously, uniaxially, and homogeneously compressed to the volume of the final state, and then it is relaxed to the final internal energy on the shock Hugoniot by time-reversible integral feedback. Because the method focuses on the final state, rather than the full propagation of the shock wave, longer times in the relaxation process can be followed using more accurate semiempirical or *ab initio* descriptions of the interatomic interactions. A comparison with NEMD simulations of Lennard-Jones single crystals shocked along the ⟨100⟩ direction has shown that the Hugoniostat reproduces not only the shock Hugoniot over a wide range of densities, but also the defect structures and final temperatures (which are unavailable from experiments on optically opaque

materials).[13] In addition, its implementation in *ab initio* molecular-dynamics methods is straightforward and has recently been used to obtain the shock Hugoniot of tin up to 200 GPa.[14] In this paper, we will employ the moniker "NVHug," when referring to this uniaxial constant-volume (or constant-strain) Hugoniostat, since the number of particles N and the periodic, uniaxially compressed computational cell of volume V are both held constant, while the internal energy is "ergostatted" to its final Hugoniot value.

A drawback of the method, however, is the way in which the uniaxial deformation is applied to the system. Because the system is instantaneously compressed, the initial temperature and stresses can become unrealistically large, in particular at very high compressions (strains). These initial large transients can lead to differences between the shock states produced by the NVHug Hugoniostat and those produced via full NEMD simulations, as will be demonstrated below.

The passage of a shock wave imposes a finite strain rate on the system. However, in the NVHug formalism the applied strain rate is effectively infinite. One way to circumvent the anomalously large transients resulting from the Hugoniostat's instantaneous uniaxial compression is to apply the deformation over a finite amount of time. This can be accomplished by imposing the strain at a constant rate, which brings the system more gradually to the final compressed volume. At that point, the same NVHug feedback dynamics can be employed. The magnitude of the strain rate can be related to that imposed at the shock front.

Recently Reed *et al.*[15] have proposed an equilibrium molecular-dynamics method for simulating shocked states in which the length of the computational box in the shock direction is modified dynamically, rather than instantaneously, as is done in the NVHug formulation. Instead of the final strain or pressure, they choose the shock velocity as the constraint parameter in determining the final equilibrium volume along the Hugoniot. However, like the Hugoniostat, the method exhibits large initial transients in stress as well as in volume. In addition, it displays long-lived volume oscillations that are qualitatively unlike the corresponding NEMD shock-wave profiles[16] and that also make an accurate determination of phase changes along the Hugoniot more difficult.

In this paper we improve upon the original Hugoniostat equations of motion in order to take into account the finite strain-rate dependence inherent in the shock front and to remedy some of the shortcomings discussed above. In this new formalism, the system is uniaxially and homogeneously compressed—not instantaneously, but rather, dynamically—to a final preset normal-stress value. This is accomplished by introducing into the Hugoniostat equations of motion an extra dynamical, integral-feedback ("barostat") variable, namely the strain rate, which acts like a piston, compressing the system uniaxially and homogeneously to a final normal stress (or normal pressure) P_{zz} in the direction (z) of the shock. In this approach, the stresses and temperature evolve dynamically and naturally. The large initial transients present in the NVHug method are eliminated by introducing damping rates in the equations of motion of both the strain-rate (barostat) and heat-flow (ergostat) variables. As a result, the time evolution of the stress tensor and temperature resembles very closely that generated in NEMD simulations. The internal energy relaxes to the final shocked-state (Hugoniot) energy, and the change from initial to final state is the work done by the piston plus the heat flow into the system. We will refer to this version of the constant-stress Hugoniostat by the moniker "NPzzHug," since in this approach the final P_{zz} becomes the constraint variable rather than the volume.

In the next section we outline the formalism and equations of motion and review some of the salient features of the model. As a demonstration of the method, we present results of shock propagation along the $\langle 110 \rangle$ direction of a Lennard-Jones crystal, comparing direct large-scale NEMD with the equilibrium NPzzHug method.

II. FORMALISM

For one-dimensional steady flow, the conservation of mass, momentum, and energy across a planar shock front connecting the initial (unshocked) and final (shocked) states leads to the Hugoniot relations:

$$\text{mass:} \quad \rho_0 u_s = \rho(u_s - u_p), \tag{1}$$

$$\text{momentum:} \quad P_{zz} = P_0 + \rho_0 u_s u_p, \tag{2}$$

$$\text{energy:} \quad E_H = E_0 + \frac{1}{2}(P_{zz} + P_0)(V_0 - V). \tag{3}$$

The subscript 0 in the above equations refers to those quantities in the unshocked initial state. P_{zz} is the normal component of the stress tensor in the direction of the shock wave (chosen to be in the z direction), $\rho = 1/V$ is the mass per unit volume, u_s is the shock velocity, and u_p is the particle velocity. From Eqs. (1) and (2) above, one obtains the following relations:[17]

$$\frac{u_p}{u_s} = 1 - \frac{V}{V_0} = \epsilon, \tag{4}$$

$$u_s = \sqrt{\frac{P_{zz} - P_0}{V_0 - V}} V_0, \tag{5}$$

$$u_p = \sqrt{(P_{zz} - P_0)(V_0 - V)}. \tag{6}$$

For a steady shock wave, all quantities in the final state (E, P_{zz}, V, u_s, u_p) in Eqs. (1)–(6) are well defined and uniquely identify the corresponding shocked state. The curve describing the locus of final states, plotted as a function of any pair of these quantities, defines the Hugoniot with respect to those variables.

In the NVHug method of Ref. 13, the traditional molecular-dynamics equations of motion of a system of N particles with coordinates $\mathbf{r}_i$ and momenta $\mathbf{p}_i$ are augmented by the addition of one extra degree of freedom, namely, the dimensionless heat-flow variable ζ that is used to relax the instantaneous internal energy E of the system to the Hugoniot energy given in Eq. (3): $E_H(t) = E_0 + \frac{1}{2}[P_{zz}(t) + P_0](V_0 - V)$. The equilibration employs integral feedback analogous to the constant-temperature molecular-dynamics method of

Nosé[18] but cast in the simplified formulation of Hoover.[19] We write the equations of motion as follows:[20]

$$\dot{r}_{\alpha i} = \frac{p_{\alpha i}}{m_i}, \tag{7}$$

$$\dot{p}_{\alpha i} = F_{\alpha i} - \nu_H \zeta p_{\alpha i}, \tag{8}$$

$$\dot{\zeta} = \frac{\nu_H}{B_0 V_0}[E - E_H(t)]. \tag{9}$$

The subscript α refers to Cartesian components (x,y,z). The energy difference in the dynamical evolution of the dimensionless heat-flow variable ζ [Eq. (9)] has been normalized by the bulk modulus at zero pressure B_0 times the zero-pressure volume V_0, since the variation of the internal energy with compression depends strongly on the compressibility of the material. The heat-flow coupling rate (frequency) ν_H is a constant that provides the time scale for the heat flow. Because ζ couples only to the momenta of the particles, the internal energy is in fact relaxed by adjusting the kinetic temperature of the system, assuring that the final temperature is correct for the shocked state characterized by the final volume V.

We have modified these equations by introducing an extra degree of freedom, a "piston" or dimensionless strain-rate variable η_z, whose role is to equilibrate the component of the stress tensor in the shock propagation direction to the desired value (P_{zz}). The implementation of this uniaxial "barostat" into the NVHug equations of motion (7)–(9) closely follows the isobaric-isothermal molecular-dynamics prescription of Hoover[21] with the modifications introduced by Melchionna *et al.*:[22]

$$\dot{r}_{\alpha i} = \frac{p_{\alpha i}}{m_i} + \nu_p \eta_\alpha r_{\alpha i}, \tag{10}$$

$$\dot{p}_{\alpha i} = F_{\alpha i} - (\nu_p \eta_\alpha + \nu_H \zeta) p_{\alpha i}, \tag{11}$$

$$\dot{L}_\alpha = \nu_p \eta_\alpha L_\alpha, \tag{12}$$

$$\dot{\zeta} = \frac{\nu_H}{B_0 V_0}[E - E_H(t)] - \beta_H \zeta, \tag{13}$$

$$\dot{\eta}_\alpha = \frac{\nu_p}{B_0}(\sigma_{\alpha\alpha} - P_{\alpha\alpha}) - \beta_p \eta_\alpha, \tag{14}$$

where $\sigma_{\alpha\beta} = \Sigma(p_{\alpha i} p_{\beta i}/m_i + r_{\beta i} F_{\alpha i})/V$ is the internal stress tensor and now $E_H(t) = E_0 + \frac{1}{2}[\sigma_{zz}(t) + P_0][V_0 - V(t)]$. For simplicity, the equations have been written in a compact form, where it is understood that $\eta_\alpha \equiv 0 \equiv \dot{\eta}_\alpha$ for $\alpha = x,y$. There is only one strain-rate variable η_z that dynamically modifies the length of the computational box in the shock direction L_z [Eq. (12)] and adjusts the instantaneous normal component of the stress tensor $\sigma_{zz}(t)$ to the preset value P_{zz} [Eq. (14)]. The heat-flow (ergostat) Eq. (13) and strain-rate (barostat) Eq. (14) include coupling-rate parameters (frequencies) ν_H and ν_p, as well as damping coefficients β_H and β_p, respectively. Damping has been incorporated in order to eliminate unrealistically large initial transients in temperature and stress, to make the time evolution of the stress tensor and temperature more closely resemble that produced by the passage of a shock wave, and to reduce thereby the errors in determining phase transition boundaries.

Equations (10)–(14) form a closed set of coupled differential equations that can easily be integrated. Starting from an initial unshocked state at pressure P_0 (usually zero), temperature T_0, volume V_0, and internal energy E_0, the system is dynamically and uniaxially compressed to the desired normal pressure P_{zz} within a natural relaxation time that is inversely proportional to the barostat frequency ν_p. Ideally, ν_p should be chosen so as to reproduce as closely as possible the strain rate produced by the passage of an NEMD shock wave through the medium. Even though the long-time average of the normal stress σ_{zz} is independent of the choice of ν_p and β_p, the density of defects in the plastic deformation depends somewhat on the strain rate imposed on the system. The final temperature, in turn, depends upon the plastic work done on the crystal. Selecting appropriate values of ν_p and β_p helps, in practice, produce better agreement between the final states and shock temperatures obtained using NPzzHug and those resulting from traditional NEMD simulations. Computational details and other features inherent in the model are discussed in the next section with the help of a numerical example.

III. NUMERICAL EXAMPLE

We have chosen to study, as an example of the NPzzHug method, the Hugoniot of a Lennard-Jones crystal shocked along the $\langle 110 \rangle$ direction. This crystallographic direction is known to have a large value of the normal stress at the Hugoniot elastic limit (HEL).[8] All simulations reported here were performed on systems containing 25 200 atoms interacting via a Lennard-Jones LJ 6-12 spline potential as described in Ref. 23. The computational cell is approximately a cube of size $18 \times 25 \times 28$ unit cells, with the x, y, and z axes oriented along $\langle 001 \rangle$, $\langle 1\bar{1}0 \rangle$, and $\langle 110 \rangle$, respectively. Periodic boundary conditions were employed in all three directions. All quantities are expressed in Lennard-Jones units: masses are given in units of the atomic mass m, lengths in units of the bond distance r_0, and energies in units of the bond energy ε_0; as a result, time is in units of $t_0 = r_0(m/\varepsilon_0)^{1/2}$, temperature in units of ε_0/k_B (k_B is Boltzmann's constant), and pressure in units of ε_0/r_0^3. The equations of motion are numerically integrated using Størmer finite differences (leap-frog) with a time step $dt = (0.002 - 0.005)t_0$.

The initial unshocked state is taken to be a perfect fcc crystal at $P_0 = 0$ and $T_0 = 0.01$, where $\rho_0 = 1.469$, $E_0 = -6.334$, and $B_0 = 81.8$. We employ the same criterion as in Ref. 13 for selecting an optimal value for the heat-flow rate ν_H, namely that it should be close to either the Einstein frequency or mean natural vibrational frequency of the atoms. This frequency increases with compression. Typical values for ν_H employed in the simulations reported here are in the range $(30 - 60)t_0^{-1}$. The damping rate β_H was chosen so that the heat flow variable ζ in Eq. (13) is critically damped, which gives $\beta_H = 2\nu_H$.

The barostat frequency ν_p is selected by equating the maximum strain rate imposed by the piston to the strain rate inherent in a shock wave of the same strength, which, for shock-wave thickness λ, is given by $\dot{\epsilon}=u_p/\lambda$. The shock thickness can be obtained from NMED profiles of particle velocity, density, or stress (normal or shear). For weak shocks along the $\langle 100\rangle$ direction, the strain rate as a function of pressure has been found[3] to closely follow a power law of the form $\dot{\epsilon}t_0=\alpha(P/\rho_0 c_0^2)^m$, where c_0 is the longitudinal sound speed at zero pressure, $m\approx 3.3$, and $\alpha\approx 1$. From Eq. (14), the maximum strain rate is

$$\dot{\varepsilon}_{max}=\nu_p\eta_{max}\approx-\nu_p\frac{P_{zz}}{B_0}. \tag{15}$$

For normal pressures in the range $P\approx B_0$, the strain rate is $|\dot{\epsilon}|\approx 1$, which implies that $\nu_p\approx 1$. We chose values of $\nu_p=0.5-1.0$ for the simulations reported here.

The damping rate constant β_p was chosen so that the strain-rate variable η_z is critically damped. An effective harmonic frequency in the strain-rate equations of motion can be obtained by expanding σ_{zz} in Eq. (14) around its equilibrium preset value P_{zz}. The resulting equation of motion is that of a damped harmonic oscillator with an effective frequency Ω given by

$$\Omega^2=\nu_p^2\frac{C_{33}+C'_{33}P_{zz}}{B_0}, \tag{16}$$

where C'_{33} is the pressure derivative of C_{33}. In the elastic regime, and for compression along $\langle 110\rangle$ direction, $C_{33}=156$ and $C'_{33}=13.9$. Employing these values in Eq. (16) above and setting $\beta_p=2\Omega$ gives the variation of the damping rate with compression. For $\nu_p=1$, $\beta_p=5-15$ for P_{zz} in the range 40–300.

Figure 1 shows the time evolution of both the normal and shear stress from damped and undamped simulations. In both sets of runs, the system was shocked to a final normal pressure $P_{zz}=40$. This target normal pressure is just below the HEL of this system ($P_{zz}^{HEL}=41$). Damping reduces the large initial fluctuations present in the undamped simulations and therefore helps determine more accurately critical values near a phase transition. As depicted in Fig. 1, in the undamped system the elastic-plastic transition can occur at a lower normal pressure than the HEL value due to large transient fluctuations, leading to errors in the determination of the HEL transition pressure. Moreover, when critical damping is included in an NPzzHug simulation, the resulting time series (as in Fig. 1) resembles much more closely the corresponding NEMD shock-wave profile.

A. Work and heat flow

In the NPzzHug formalism, the internal energy $E=K+\Phi$ (kinetic plus potential) changes dynamically with time, with a rate of change that can be be related to the work done by the piston in compressing the system to the desired pressure ($-W$) and the heat flow into the system (Q):

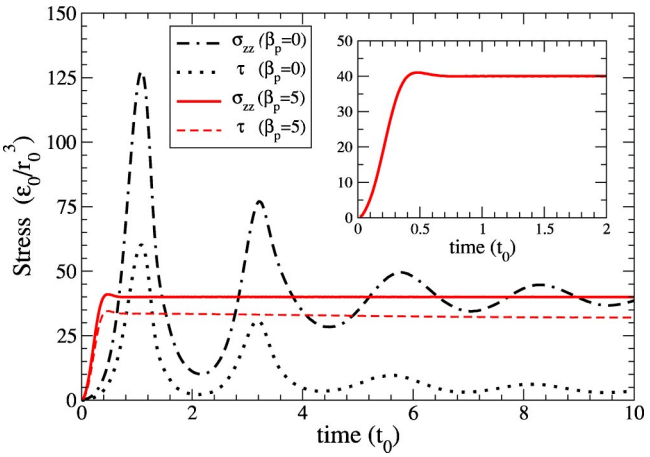

FIG. 1. (Color online) Time evolution of normal stress σ_{zz} and shear stress $\tau\,[2\tau=\sigma_{zz}-(\sigma_{xx}+\sigma_{yy})/2]$ for a 25 200-atom LJ crystal shocked along the $\langle 110\rangle$ direction to a normal pressure $P_{zz}=40$, close to the Hugoniot elastic limit (HEL) for this crystallographic direction ($P_{zz}^{HEL}=41$). The molecular-dynamics equilibration to this final state has been done for two cases: no damping ($\beta_H=0=\beta_p$) and with damping ($\beta_H=30,\beta_p=5$). In both cases, the rate parameters have been set to $\nu_H=30$, $\nu_p=1$. The large initial fluctuations, evident in the undamped case, lead to plastic deformation below the actual HEL with an accompanying reduction in the shear stress. No plastic deformation is observed in the damped case. The inset shows the early time evolution of the normal stress for the damped case, which reaches the target equilibrium value at significantly earlier times than the undamped case.

$$\dot{E}=\dot{Q}-\dot{W}, \tag{17}$$

where

$$\dot{E}=\sum_i^N m_i\mathbf{v}_i\cdot\dot{\mathbf{v}}_i-\sum_i^N\mathbf{F}_i\cdot\dot{\mathbf{r}}_i. \tag{18}$$

Using Eqs. (10) and (11), this can be expressed in terms of the heat-flow and strain-rate variables ζ and η_z:

$$\dot{E}=-3Nk_BT\nu_H\zeta-\sigma_{zz}V\nu_p\eta_z. \tag{19}$$

Assuming the final state is reached in time t, the change in internal energy between initial and final states $E(t)-E(0)=\Delta E=\Delta Q-\Delta W$, can be expressed in terms of integrals of the strain-rate and heat-flow variables over the simulation time:

$$\Delta Q=-3Nk_B\nu_H\int_0^t dt'\zeta(t')T(t'), \tag{20}$$

$$\Delta W=\nu_p\int_0^t dt'\,\eta_z(t')\sigma_{zz}(t')V(t'). \tag{21}$$

Figure 2 shows a typical trajectory of normal stress as a function of volume. The work done by the piston, given by the integral in Eq. (21) above, is equal to the area under the curve. From the Hugoniot conservation laws, the work done by a steady shock in compressing the material from initial state (P_0,V_0,E_0) to final state (P_{zz},V,E) is given by the area

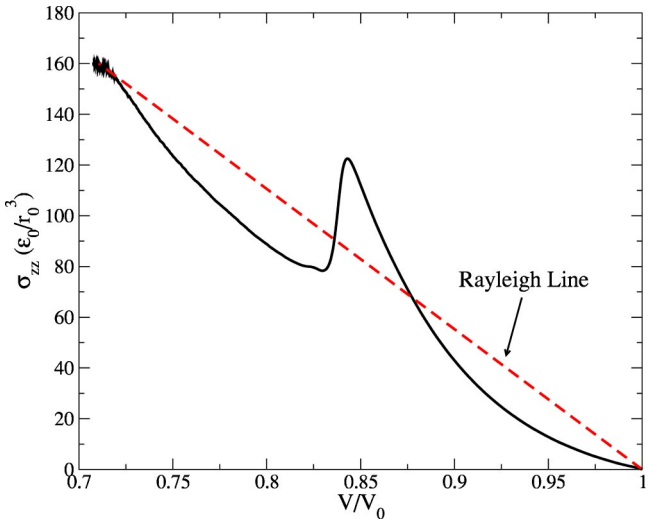

FIG. 2. (Color online) NPzzHug trajectory of normal stress σ_{zz} as a function of volume V from a simulation in which the target $P_{zz}=160$. Also shown is the Rayleigh line connecting the initial and final states. The final state is in the overdriven region of the Hugoniot. The hump in the trajectory is caused by initial overshoot of the HEL followed by plastic deformation.

under the Rayleigh line, the straight line in $P_{zz}-V$ space connecting the initial and final states [cf. Eq. (3)]: $\Delta E = \frac{1}{2}(P_{zz}+P_0)(V_0-V)$. In the present formalism, this conservation relation is satisfied by construction. Figure 3 shows the time evolution of the heat flow ΔQ and work ΔW for same simulation whose σ_{zz}-V diagram is shown in Fig. 2. The curves have been obtained by numerically integrating Eqs. (20) and (21). As expected, most of the change in internal energy (about 90%) is due to the work done by the strain-rate (piston) variable, while the heat-flow variable ensures that final shock Hugoniot temperature is achieved.

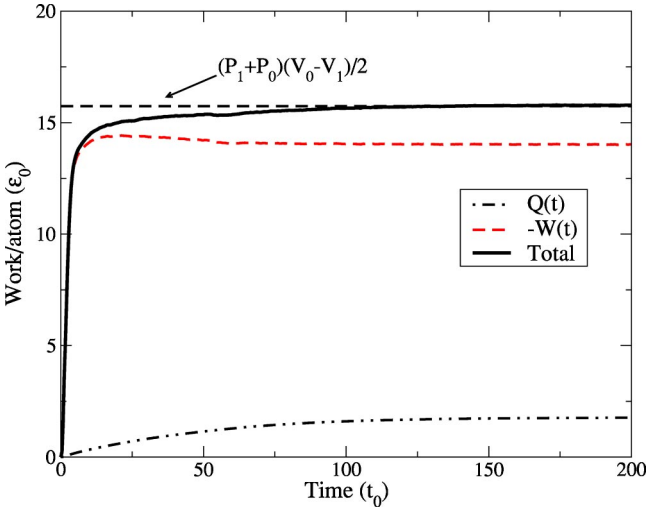

FIG. 3. (Color online) Heat into the NPzzHug system ΔQ and work done by the piston $-\Delta W$ as a function of time, as obtained from numerically integrating Eqs. (20) and (21), respectively. The sum of the two terms is equal to $\Delta E=\frac{1}{2}(P_1+P_0)(V_0-V_1)$. Most of this energy change ($\approx$90%) is due to the work done by the piston.

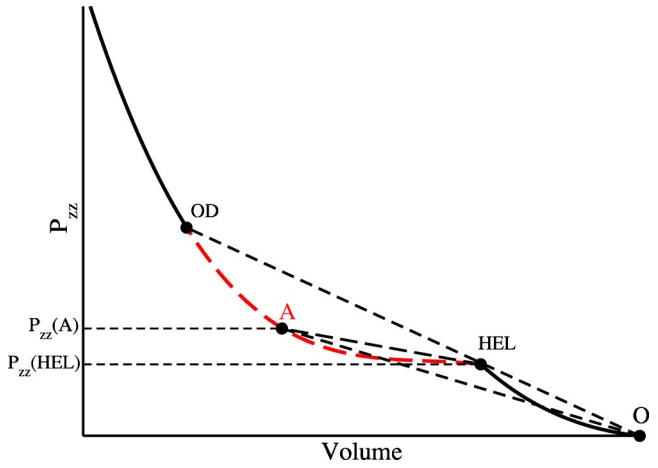

FIG. 4. (Color online) A generic Hugoniot. The dashed curve between the Hugoniot elastic limit (HEL) and the overdriven (OD) points is a region of the Hugoniot inaccessible from the initial state O. It is characterized by an elastic wave traveling at u_s^{HEL} (O-HEL line) and a plastic wave whose velocity $u_s<u_s^{HEL}$.

This exercise in thermodynamic bookkeeping demonstrates why it is so important to include ergostatting in the Hugoniostat formalisms, even while barostatting at a finite rate. Not all the Hugoniot energy change is strictly P-V work, as it would appear from Eq. (3). If that were so, one might be tempted to conclude that the process of shock compression is isentropic. Figure 3 shows, however, that the transient heat flow in the shock front from hot shocked to cold unshocked material is clearly nonzero, so that entropy increases, and temperature in shock compression to a given volume is higher than in the corresponding isentropic compression.

IV. PHASE CHANGES: ELASTIC-PLASTIC TRANSITION

The plastic deformation that accompanies an elastic-plastic transition, while not rigorously a structural phase change, can similarly cause a two-wave structure to develop, namely, an elastic precursor followed by a plastic wave. Figure 4 shows a generic Hugoniot. The region of the Hugoniot between the HEL and overdriven (OD) points, indicated by the dashed curve, corresponds to shock states inaccessible from the initial state (O). Shock states in this region, such as point A, are characterized by a two-wave structure: an elastic wave that compresses the material up to the HEL and travels with a velocity u_s^{HEL}, and a plastic wave that compresses the material from the HEL to A and travels at $u_s<u_s^{HEL}$. Slopes of the straight P-V lines (known as Rayleigh lines) are proportional to the square of the wave speeds [see Eq. (5)]: $P_{zz}=P_0+(u_s/V_0)^2(V_0-V)$. The plastic wave speed u_s increases with shock compression until $u_s=u_s^{HEL}$. This condition defines the OD point. For compressions above the OD, the plastic wave speed exceeds the elastic, resulting in single plastic-wave states.

As an example of phase changes and identification of transition boundaries, we have investigated the elastic-plastic transition in the LJ system shocked along the ⟨110⟩ direction.

TABLE I. NPzzHug HEL (calculated) and initial (zero-pressure), quantities for the LJ system shocked along the ⟨110⟩ direction. These values, together with the bulk modulus B_0, are parameters used in Eqs. (3) and (13) to obtain the Hugoniot.

	Initial state	HEL
Energy/atom	−6.3340	−4.9905
Volume/atom	0.6807	0.6142
Temperature	0.0100	0.1314
Pressure	0.0	41.0

A series of equilibrium Hugoniostat simulations were performed for shock normal-pressure values in the range $P_{zz}=10-340$. In the plastic regime, the system was allowed to evolve in time for about $(100-200)t_0$. In the elastic regime, however, the system reaches equilibrium very quickly, and simulation times of less than $20t_0$ are sufficient. Time averages of all relevant thermodynamic quantities were performed after allowing sufficient time for steady-state equilibration [usually within $(20-50)t_0$]. Standard deviations of the computed averaged values in temperature and density were typically of the order $\Delta T/T \leqslant 0.005$ and $\Delta\rho/\rho \leqslant 1.2\times10^{-4}$ over the range of pressures reported here.

We find that along the ⟨110⟩ direction, Lennard-Jonesium yields at compressions above ~9% with a transition characterized by a large volume collapse $\Delta V/V_0$ of 7.7%. The HEL is easily identified by a drop in the computed shock velocity, accompanied by plastic deformation for shock pressures above the HEL. Due to plastic work, the plastic deformation results in a jump in temperature, which can be easily monitored as a function of time. A decrease in computed wave speed with increase in pressure is caused by either a reduction in the compressibility of the material with increase in density, or else regions of the Hugoniot that exhibit a negative curvature, i.e., concave downwards ($d^2P/dV^2<0$), indicating a phase change. For the shock wave to be stable, the shock velocity must increase with pressure. Since the square of the shock velocity is proportional to the slope of the Rayleigh line connecting initial and final states in the P_{zz}-V plane, those lines connecting the zero-pressure state with states in the two-wave region of the Hugoniot, such as point A in Fig. 4 (O-A dashed line), have lower slopes than the line connecting the initial state with the HEL (O-HEL line). Once the HEL is determined, the plastic states in the two-wave region are obtained by recentering the initial state of the system at the HEL rather than at the zero-pressure state. Table I shows the pressure, volume, temperature, and energy values at the HEL obtained from the simulations, as well as their values at the initial (zero-pressure) state.

In order to check the accuracy of the equilibrium molecular-dynamics results, we carried out multimillion-atom NEMD simulations in the elastic-plastic region of the Hugoniot. The simulations involved up to 49 million atoms arranged in a perfect fcc ⟨110⟩ rectangular crystal slab with up to 10 000 atomic planes in the shock propagation direction (z direction) and periodic boundary conditions in the transverse (x and y) directions. The procedure used to initiate a shock wave of a given strength is detailed in Ref. 3: the crystal is hurled towards an infinitely massive piston with a velocity $-u_p$, which produces a shock wave that propagates away from the piston with velocity u_s-u_p. Thermodynamic quantities are obtained by spatial averaging over 3000 atomic planes, excluding the first 1000 planes near the piston.

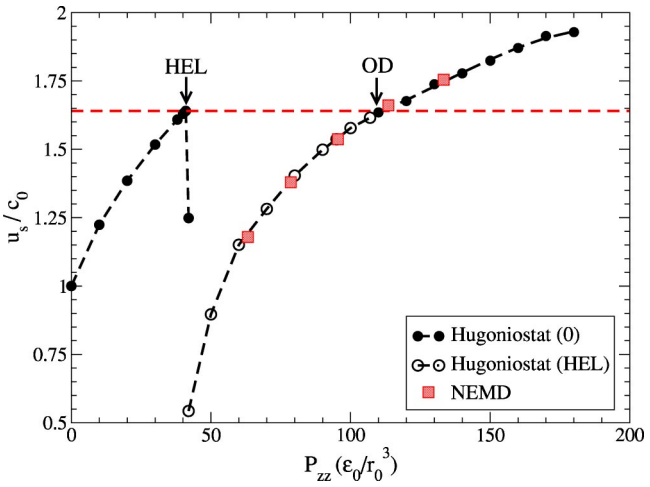

FIG. 5. (Color online) NPzzHug and NEMD shock velocity u_s (normalized by the zero-pressure longitudinal sound speed $c_0=10.3$) vs P_{zz} in fcc ⟨110⟩-direction shocks. Label (0) indicates system started from initial zero-pressure state, while (HEL) refers to states obtained from re-centering at the HEL. The horizontal dashed line has been drawn to help identification of the OD point, where the plastic wave speed equals u_s^{HEL}.

Figure 5 shows computed shock velocities as a function of P_{zz}, from Hugoniostat and NEMD simulations. In the elastic regime, the shock velocity increases with normal pressure up to the HEL. The first point beyond the HEL (filled circle) does not correspond to a physical shock state, rather it has been included to show how a decrease in shock velocity computed from the zero-pressure state serves to identify the elastic limit of the Hugoniot, which in this system is at $P_{zz}^{HEL}=41$. For normal pressures larger than P_{zz}^{HEL}, but below the OD regime, the shock states are characterized by a two-wave structure: an elastic wave with velocity u_s^{HEL} and a plastic wave that travels at $u_s<u_s^{HEL}$. The plastic states in the two-wave region, indicated by open circles in Fig. 5, are obtained by recentering the initial state to the HEL instead of the zero-pressure state. The values of the thermodynamic variables (temperature, pressure, density) that define the initial state recentered at the HEL are indicated in Table I. The plastic-wave speed increases with normal pressure until it is equal to the HEL elastic-wave speed u_s^{HEL} at the OD point. For compressions beyond the overdriven point, the plastic-wave speed is larger than the elastic, resulting in single plastic-wave states obtained from the initial zero-pressure state (O). As seen in Fig. 5, the Hugoniostat results are in very good agreement with the much more computationally intensive NEMD simulations in the two-wave and overdriven regimes.

Figure 6 shows the computed shock velocities as a function of particle velocity from NPzzHug and NEMD simulations. The open circles indicate plastic-wave shock velocities

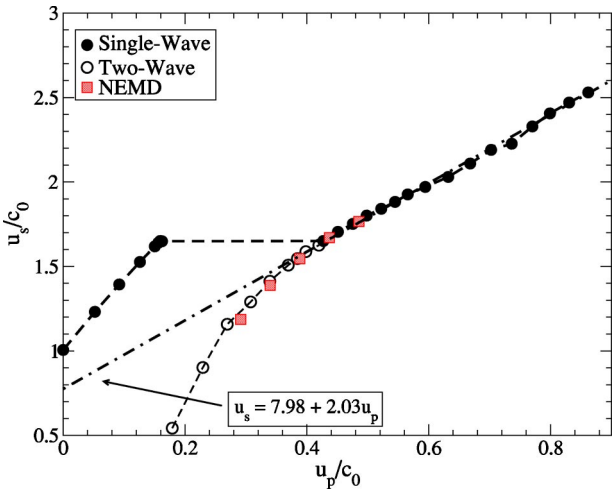

FIG. 6. (Color online) NPzzHug and NEMD shock velocities u_s as a function of particle velocity u_p normalized to the longitudinal sound speed at zero pressure ($c_0=10.3$). Also shown is a linear u_s-u_p fit using the Hugoniostat data points above the OD: $u_s=7.98+2.03u_p$.

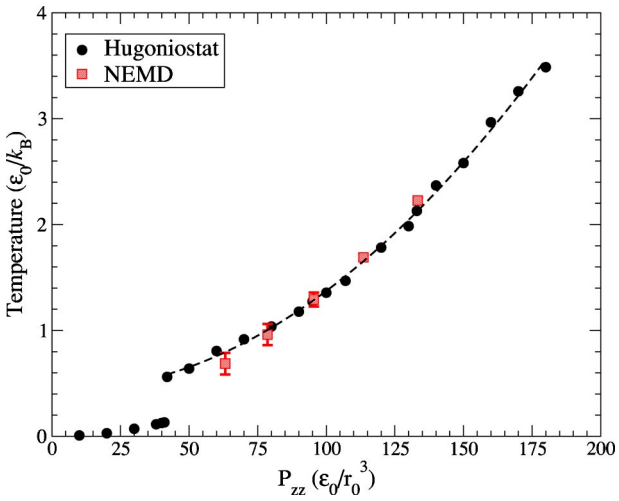

FIG. 7. (Color online) Comparison between NEMD and NPzzHug shock temperature as a function of normal P_{zz}.

in the two-wave region while the solid circles are single-wave states, either elastic (below HEL) or plastic (above OD). Even though they are not drawn, for each plastic wave in the two-wave region, there exists an elastic wave that travels at u_s^{HEL}.

It is common to describe the u_s-u_p Hugoniot by a linear relation of the form $u_s=c+su_p$, where c is the zero-pressure shock velocity and the slope s can be related to the pressure derivative of the bulk modulus at zero pressure. A linear fit of the Hugoniostat data above the OD gives $c=7.98$ and $s=2.03$, shown in Fig. 6. In general, the high-pressure u_s-u_p data should extrapolate to the zero-pressure bulk sound speed c_B, indicating that the high-pressure states are isotropic. For this system, $c_B=(B_0/\rho_0)^{1/2}=7.46$, which is lower than c. This might indicate a phase change, in which the compressibility of the material has increased, or that the high-pressure states exhibit residual shear stress and are not completely isotropic, as is the case here.

A. Shock temperatures

Figure 7 shows NEMD and Hugoniostat shock temperatures as a function of P_{zz}. A discontinuous jump in temperature occurs at the HEL and indicates a transition from elastic to plastic states. Most of the NEMD simulations were done in the two-wave region (between the HEL and OD in Fig. 5). This region is the most sensitive to defect densities, since it is closest to the HEL. In either version of the Hugoniostat—constant-volume or constant-stress—shock temperatures in the two-wave region depend on the value of the state variables ($E_{HEL}, V_{HEL}, P_{HEL}$) at the HEL. They are also strongly dependent on system size, since too small a system will not be able to capture the appropriate defect densities, which increase with strain rate and shock strength.[3] The good agreement between NEMD and Hugoniostat temperatures indicate that the system size used in both kinds of Hugoniostat simulations is sufficient to capture correctly the defect structures, and also that the HEL has been correctly identified (see Table I).

It should be noted that such good agreement for shock temperatures from the Hugoniostat would not be possible, especially for strong shocks, if the heat flow were turned off ($\nu_H \equiv 0$). Then, temperatures would be lower, more nearly resembling those observed in isentropic compression.

B. Comparison with the constant-volume Hugoniostat

We also carried out simulations of Lennard-Jones fcc $\langle 110 \rangle$ shock states using the constant-volume Hugoniostat[13] (NVHug) for the same system size and initial conditions used in the constant-stress method, setting $\nu_p=\beta_p=\beta=0$ in the NPzzHug Eqs. (10)–(14). The normal-pressure versus volume Hugoniot is shown in Fig. 8. As already noted, the elastic-plastic transition is characterized by a volume collapse $\Delta V/V_0$ of 7.7%. The region between V_{HEL} and $(V_{HEL}-\Delta V)$ is an unstable region with low compressibility. Since the volume cannot change in the NVHug formalism, temperatures and pressures computed in the unstable region will exhibit anomalously low values, as shown in Fig. 8. A series of NVHug simulations is therefore necessary in order to correctly assess the transition volume change, and to determine the corresponding stable regions of the Hugoniot by finding the compression at which the normal pressure equals the HEL value. In constrast, the NPzzHug formalism yields only stable states with increasing normal pressure.

One major difference between the two methods is in the way the deformation is applied to the system. In the constant-volume method, the uniaxial deformation is applied homogeneously and instantaneously. This creates unwanted initial transients in both temperature and stress (normal and/or shear) that increase with compression. In constrast, the constant-stress version presented here produces no transients in either temperature or pressure, and by design, the imposed strain rate is approximately equal to that produced by a shock wave of the strength being simulated.

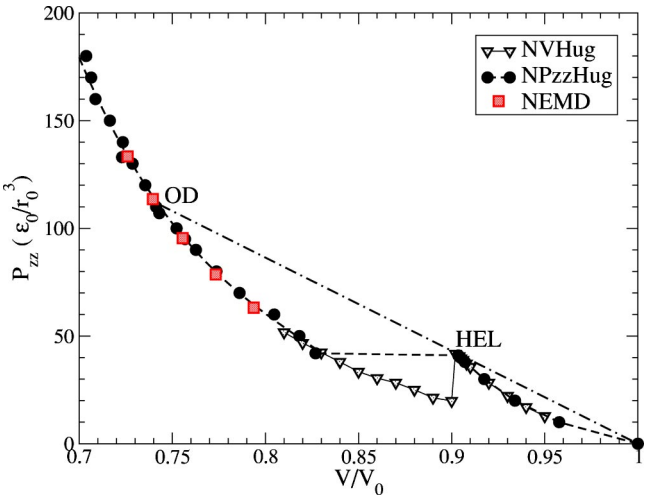

FIG. 8. (Color online) NPzzHug, NVHug, and NEMD normal pressure P_{zz} vs volume of the LJ system shocked along the $\langle 110 \rangle$ direction. NVHug simulations (triangles) in the unstable region of the Hugoniot give equilibrium temperatures and normal pressures below those at the HEL. Several simulations are required in order to identify the stable region beyond the HEL, where $P_{zz} \geqslant P_{zz}^{HEL}$. In constrast, NPzzHug gives only stable phases along the Hugoniot curve. Both methods agree well with NEMD simulations.

The effect of these large initial transients on the damaged state in the NVHug method can be significant, in particular at large compressions. Figure 9 shows cross-sectional views (about 6 $\langle 110 \rangle$ planes thick) of the atomic configuration from NVHug, NPzzHug, and NEMD simulations with about the same uniaxial compression (26%). The structure produced by NVHug [Fig. 9(a)] is not liquid, but rather, amorphous. The amorphization is produced by the very large initial shear stress imposed on the system under instantaneous compression. It should be noted that at this compression, the material is very far from the melt line. In constrast, no such amorphization is seen in the NPzzHug method at any of the simulated normal pressures reported here. Furthermore, the structural deformation and defects densities produced in the NPzzHug simulations [Fig. 9(b)], are in close agreement with those produced in the NEMD simulations [Fig. 9(c)].

In summary, the structure resulting from an instantaneous compression in NVHug might show marked differences with those produced by the passage of a shock wave and its finite strain rate. The constant-stress Hugoniostat incorporates strain-rate dependence naturally, and it is therefore better able to reproduce the damaged states produced in shock waves.

V. CONCLUSIONS

The strain rates inherent in shock waves, while large, are finite. The constant-stress Hugoniostat formulation introduced here takes this into account. A strain-rate (barostat) variable acts as a piston, compressing the computational box in the shock direction at a finite rate like that at the shock front, while a heat flow (ergostat) variable relaxes the internal energy to the final shocked-state value. By incorporating

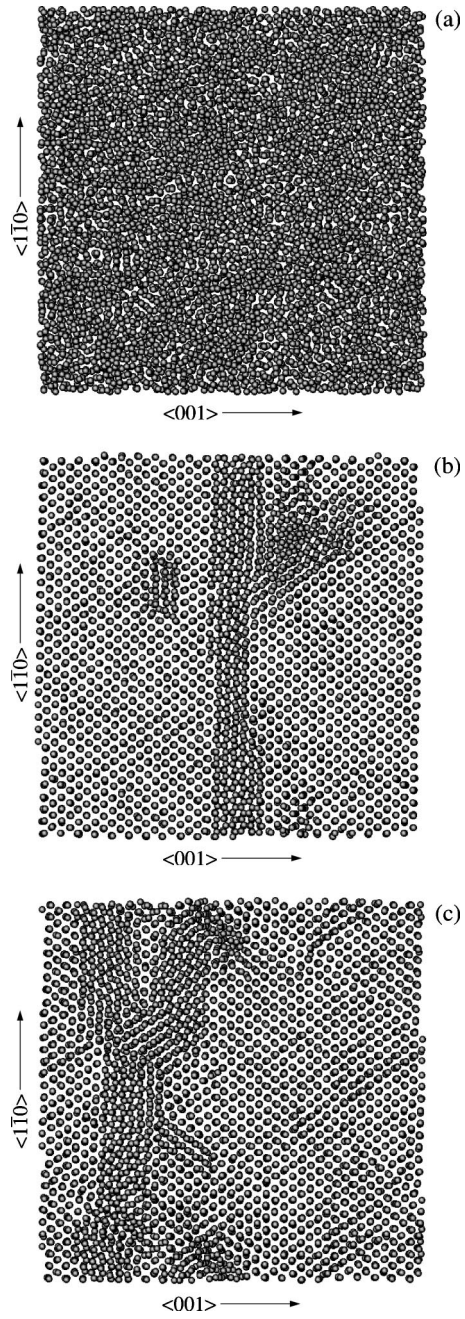

FIG. 9. Cross-sectional profiles ($25 \times 25 r_0^2$) of atomic configurations at 26% compression from three types of simulations: (a) NVHug (Ref. 13), (b) NPzzHug, and (c) NEMD. The structure shown in (a) is not melted, but amorphous. The instantaneous compression in NVHug produces very large initial shear stress values and results in amorphization on a short time scale (within $2t_0$). In constrast, no such amorphization is seen in NPzzHug (b) or NEMD (c) simulations over the entire range of normal pressures reported here (i.e., below shock-induced melting). In addition, the observed structural deformation in the NPzzHug simulations closely resemble those produced in large-scale NEMD simulations.

critical damping in the barostat and ergostat variables, large overshoots in stress and temperature (which can artificially induce plasticity or phase changes) are eliminated, and the time profiles of pressure and temperature resemble more

closely those produced in NEMD simulations. As a result, the plastic damage produced by the NPzzHug method is indistinguishable from full-scale NEMD simulations, as is the final temperature at the shocked (Hugoniot) state, provided the system size is sufficiently large to correctly capture defect densities.

Ergostating has been shown to be necessary in order to correctly reproduce shock temperatures. Shock waves are intrinsically a nonhomogeneous, nonlinear phenomena. It is not possible, within an equilibrium molecular-dynamics formulation, to exactly reproduce the stress and density gradients present at the shock front. Hence, it is necessary to supplement the work done by the barostat with the right heat flow, controlled by the ergostat.

In summary, the NPzzHug method overcomes the limitations of other methods, without increasing the computational effort. We have demonstrated here that, together with NEMD, NPzzHug is a robust method for mapping out the shock response of condensed matter, even for the case of multiple waves.

ACKNOWLEDGMENTS

Part of this work was supported by the U.S. Department of Energy under Contract No. W-7405-ENG-36.

[1] A. Paskin and G. J. Dienes, J. Appl. Phys. **43**, 1605 (1972); B. L. Holian and G. K. Straub, Phys. Rev. Lett. **43**, 1598 (1979).
[2] B. L. Holian, W. G. Hoover, B. Moran, and G. K. Straub, Phys. Rev. A **22**, 2798 (1980).
[3] B. L. Holian and P. S. Lomdahl, Science **80**, 2085 (1998).
[4] K. Kadau, T. C. Germann, P. S. Lomdahl, and B. L. Holian, Science **296**, 1681 (2002).
[5] B. L. Holian, T. C. Germann, J.-B. Maillet, and C. T. White, Phys. Rev. Lett. **89**, 285501 (2002).
[6] T. C. Germann, in *Shock Compression of Condensed Matter—2001*, edited by M. D. Furnish, Y. Horie, and N. N. Thadhani AIP Conf. Proc. No. 620 (AIP, Melville, 2002), p. 333.
[7] P. A. Rigg and Y. M. Gupta, Phys. Rev. B **63**, 094112 (2001).
[8] T. C. Germann, B. L. Holian, P. S. Lomdahl, and R. Ravelo, Phys. Rev. Lett. **84**, 5351 (2000).
[9] M. A. Meyers, F. Gregori, B. K. Kad, M. S. Schneider, D. H. Kalantar, B. A. Remington, G. Ravichandran, T. Boehly, and J. S. Wark, Acta Mater. **51**, 1211 (2003).
[10] D. Tanguy, M. Mareschal, P. Lomdahl, T. C. Germann, B. L. Holian, R. Ravelo, and T. C. Germann, Phys. Rev. B **68**, 144111 (2003).
[11] T. C. Germann, D. Tanguy, B. L. Holian, P. S. Lomdahl, M. Mareschal, and R. Ravelo, Metall. Mater. Trans. B (to be published).
[12] V. V. Zhakhovskii, S. V. Zybin, K. Nishihara, and S. I. Anisimov, Phys. Rev. Lett. **83**, 1175 (1999).
[13] J.-B. Maillet, M. Mareschal, L. Soulard, R. Ravelo, P. S. Lomdahl, T. C. Germann, and B. L. Holian, Phys. Rev. E **63**, 016121 (2001).
[14] S. Bernard and J.-B Maillet, Phys. Rev. B **66**, 012103 (2002).
[15] E. J. Reed, L. E. Fried, and J. D. Joannopoulos, Phys. Rev. Lett. **90**, 235503 (2003).
[16] E. J. Reed (private communication).
[17] Ya B. Zel'dovich and Yu P. Raizer, *Physics of Shock Waves and High-Temperature Hydrodynamic Phenomena* (Academic, New York, 1968).
[18] S. Nosé, J. Chem. Phys. **81**, 511 (1984).
[19] W. G. Hoover, Phys. Rev. A **31**, 1695 (1985).
[20] We have chosen to write the heat-flow rate variable of Ref. 13 as $\chi = \nu_H \zeta$.
[21] W. G. Hoover, Phys. Rev. A **34**, 2499 (1986).
[22] S. Melchionna, G. Ciccotti, and B. L. Holian, Mol. Phys. **78**, 533 (1993).
[23] B. L. Holian and R. Ravelo, Phys. Rev. B **51**, 11 275 (1995).